

This document is downloaded from DR-NTU, Nanyang Technological University Library, Singapore.

Title	Selective Laser Melting Of Nickel Titanium Shape Memory Alloy
Author(s)	Khoo, Zhong Xun; Ong, C.; Liu, Yong; Chua, Chee Kai; Leong, Kah Fai; Yang, Shou Feng
Citation	Khoo, Z. X., Ong, C., Liu, Y., Chua, C. K., Leong, K. F., & Yang, S. F. (2016). Selective Laser Melting Of Nickel Titanium Shape Memory Alloy. Proceedings of the 2nd International Conference on Progress in Additive Manufacturing (Pro-AM 2016), 451-456.
Date	2016
URL	<a href="http://hdl.handle.net/10220/41806">http://hdl.handle.net/10220/41806</a>
Rights	© 2016 by Pro-AM 2016 Organizers. Published by Research Publishing, Singapore

# SELECTIVE LASER MELTING OF NICKEL TITANIUM SHAPE MEMORY ALLOY

KHOO Z.X., ONG C., LIU Y., CHUA C.K., LEONG K.F., YANG S.F.  
*School of Mechanical and Aerospace Engineering, Nanyang Technological University, 50  
Nanyang Avenue, Singapore 639798*

**ABSTRACT:** Nickel titanium (NiTi) is a type of shape memory alloy (SMA) that is difficult to process by conventional manufacturing methods. Thus, Selective Laser Melting (SLM), which is a form of additive manufacturing technology, has been proposed as a potential solution. In this paper, different NiTi samples have been fabricated by using the SLM. The laser power and laser scanning speed were varied from 10 to 100 W and from 100 to 6000 mm/s respectively while keeping the rest of the process parameters as constant. The samples with the highest bulk densities and dimensional accuracy were found to be in the range from 50 to 60 W and from 3100 to 4000 mm/s. These samples were then subjected to differential scanning calorimetry (DSC) testing to determine the presence of phase transformation.

**KEYWORDS:** 3D printing, 4D printing, additive manufacturing, selective laser melting, shape memory alloys

## INTRODUCTION

Shape memory alloy (SMA) is one type of metallic alloy that has the ability to transform thermal energy into mechanical work (Fremond & Miyazaki, 1996). This phenomenon is known as the shape memory effect (SME). SMAs are generally adopted for special engineering applications due to their SME and excellent functional properties (Dadbakhsh et al., 2014; Elahinia, Hashemi, Tabesh, & Bhaduri, 2012; H Meier, Haberland, & Frenzel, 2012). One such example is the nickel titanium (NiTi) SMA, where it can be found in applications such as biomedical implants (Bormann, Schumacher, Muller, Mertmann, & Wild, 2012; Elahinia et al., 2012; I, I., & I., 2012), smart composite materials (Sanusi, Ayodele, & Khan, 2014), actuators (Sharma, Raj, & Jangra, 2015) and micro-electromechanical systems (Sharma et al., 2015) etc.

Due to the reversible martensitic phase transformation, NiTi SMA can demonstrate both SME (thermal memory) and superelasticity (mechanical memory) (Bormann et al., 2012; Dadbakhsh et al., 2014; H Meier et al., 2012). However, this type of phase transformation is governed by the four transformation temperatures of NiTi. Furthermore, these transformation temperatures are extremely sensitive to any variation in the composition of Ni and Ti. For instance, a slight reduction in the content of Ni can lead to a huge increase in the transformation temperatures (Bormann et al., 2012; Elahinia et al., 2012; Frenzel et al., 2010; H Meier et al., 2012).

In addition to that, NiTi SMA has to be processed into various geometries to fully utilise its SME and superelasticity for the different applications. However, the conventional manufacturing processes have various flaws and NiTi is a material that is difficult to process (Elahinia et al., 2012; H. Meier, Haberland, Frenzel, & Zarnetta, 2009). Firstly, NiTi alloys are known to be compositional sensitive. When NiTi alloys are being processed under high temperature, impurity elements tend to be picked up more easily and these impurities can result in issues such as oxidation and microstructural defects. Moreover, these problems might even cause a shift in the

transformation temperatures. Second, NiTi SMA has a poor machinability. Due to the shape memory properties of NiTi alloy, it causes a significant amount of tool wear and makes it difficult for precise machining (Elahinia et al., 2012; K. Weinert & Petzoldt, 2004; H Meier et al., 2012; H. Meier et al., 2009). Additionally, conventional treatment methods such as thermomechanical treatments, annealing treatments and shape setting treatments can affect the NiTi phase transformation behavior significantly as well (Dadbakhsh et al., 2014; H. Meier et al., 2009).

Hence, to overcome these drawbacks, one method would be to produce NiTi components from NiTi powder by hot isostatic pressing (I. et al., 2012). However, this method cannot produce an object with complex geometries. Therefore, a better proposed solution would be to make use of additive manufacturing or 3D printing technologies such as Selective Laser Melting (SLM) to fabricate the NiTi components from the NiTi powder (Bormann et al., 2012; Chua & Leong, 2014; Dadbakhsh et al., 2014; I. et al., 2012; Khoo et al., 2015; H Meier et al., 2012; H. Meier et al., 2009; Shishkovsky, Yadroitsev, & Smurov, 2013; Zhang, Chen, & Coddet, 2013). This new technique of fabricating NiTi components is also known as 4D printing. 4D printing of NiTi SMA not only helps to solve the problem of poor manufacturability of NiTi alloy, it also enables the direct fabrication of NiTi smart structures with complex geometries for novel applications.

Therefore in this paper, two-dimensional (2D) NiTi SMA samples have been fabricated from NiTi powder by using a customised SLM equipment. These samples were then characterised and compared to the NiTi ingot and NiTi powder and they were shown to exhibit phase transformation.

## **EXPERIMENTAL WORK**

### **Material processing**

The NiTi powder used in this paper has an average atomic percentage of 49.91% Ni and 50.09% Ti. The powder was produced by gas atomization of NiTi ingot with a particle size ranging from 20 to 50  $\mu\text{m}$ .


To produce the NiTi samples with dimensions of 5 mm by 5 mm under the argon atmosphere, a customised SLM machine (PLS-SLM100W) was used. A thick layer of powder was deposited on the top of the aluminium base plate during the fabrication process and only the top layer of the powder bed will be melted and solidify when the laser scanned across the powder bed. There will still be a layer of powder underneath the solidified layer and the samples will not be in contact with the base plate. This method not only helps to prevent the contamination of samples due to the possible reaction between the base plate and NiTi SMA, it makes the removal of samples much easier as well. Nevertheless, the samples fabricated in this paper only consisted of a single solidified layer. Therefore, the samples produced here are considered to be 2D.

As for the process parameters, the laser power and laser scanning speed were chosen to be the variable parameters while the rest of the parameters were kept constant. The range of laser power tested was from 10 to 100 W with an interval of 10 W and the range of laser scanning speed tested was from 100 to 6000 mm/s with an interval of 100 mm/s. Table 1 presents the fixed process parameters.

### **Material characterisation**

After fabricating the 2D NiTi samples, their bulk densities were calculated by using the buoyancy method (Eq. (1)) that is based on the Archimedean Principle.

Table 1. Fixed process parameters.

Parameters	
Pitch/hatch distance	5 $\mu\text{m}$
Frequency of laser	100 kHz
Laser pulse width	10 $\mu\text{s}$
Number of time laser scanned	1
Scanning pattern	Bi-directional scanning with contour 

$$\rho_s = \rho_l \left[ \frac{m_a}{m_a - m_l} \right] \quad (1)$$

where  $\rho_s$  is the density of the NiTi sample,  $\rho_l$  is the density of the liquid used, which is temperature dependent,  $m_a$  is the mass of the sample measured in air and  $m_l$  is the mass of the sample measured after submerging in the liquid. The liquid used was deionised water and its temperature was measured to obtain its density value. Each sample was weighed in air for five times and in deionised water for five times to get an average reading of  $m_a$  and  $m_l$ .

On the other hand, the presence of the phase transformation of the NiTi ingot, NiTi powder and NiTi 2D samples were determined by differential scanning calorimetry (DSC) testing. The samples went through two cycles of heating and cooling with a ramp rate of 10  $^{\circ}\text{C}/\text{min}$  from a temperature range of -40 to 150  $^{\circ}\text{C}$ . However, only the DSC curves that correspond to the second cycle of heating and cooling processes were presented.

## RESULTS AND DISCUSSION

### Density measurement

Visual inspections were first employed to narrow down the large number of samples required for density measurement. The basic criteria used in visual inspections are that the samples must have visible melting of powder, good dimensional accuracy and minimum oxidation. Figure 1 illustrates some samples with poor melting (sintering), poor dimensional accuracy and oxidation issue. It also presents an example of a good sample for comparison.

The samples selected after visual inspections were then subjected to the measurement of their bulk densities, relative densities and closed porosities. Figure 2 shows the graphs of the different densities of the samples and their corresponding closed porosities against the laser scanning speed tested. Based on these results, the samples that were fabricated with a laser power of 50 to 60 W and with laser scanning speed of 3100 to 4000 mm/s have the highest and most consistent readings of bulk and relative densities. In other words, these samples will have the lowest closed porosities and they were chosen to undergo further testing for the presence of phase transformation.

### Phase transformation

Together with the NiTi ingot and NiTi powder, the twenty NiTi 2D samples chosen from the density measurement were put through the DSC test. The four transformation temperatures (martensitic start temperature  $M_s$ , martensitic finish temperature  $M_f$ , austenitic start temperature  $A_s$  and austenitic finish temperature  $A_f$ ) of the ingot, powder and sample with the highest bulk density

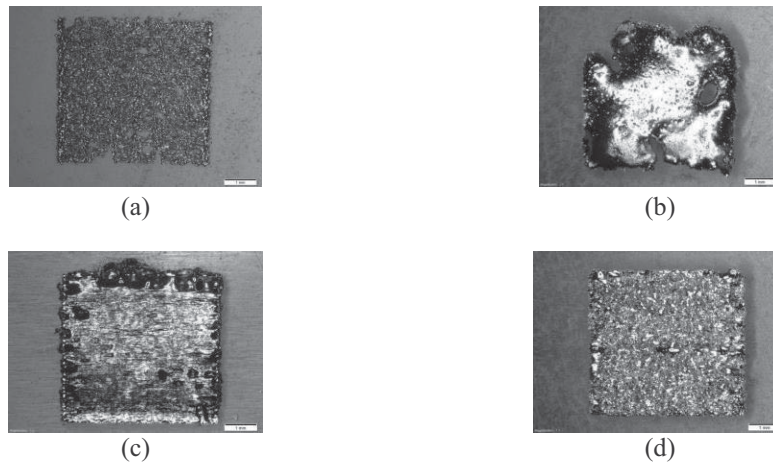


Figure 1. 2D NiTi samples with (a) poor melting, (b) poor dimensional accuracy, (c) oxidation and (d) an example of a good sample.

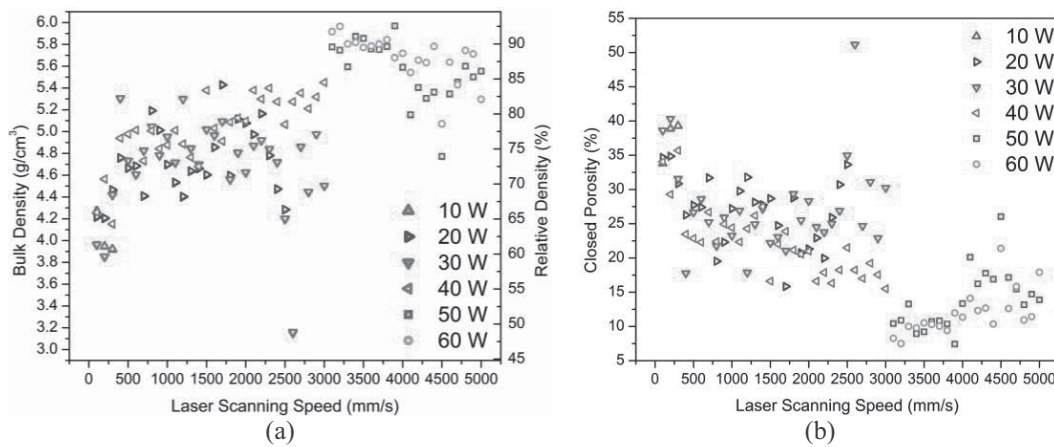


Figure 2. Results of (a) bulk densities, relative densities and (b) closed porosity of NiTi samples plotted against the laser scanning speed.

are shown in Figure 3. Figure 4 presents the comparison and trends of the four transformation temperatures of the fabricated NiTi samples with different laser powers and laser scanning speeds to that of the NiTi ingot and NiTi powder.

According to the DSC tests, all the chosen samples exhibit phase transformation during the heating and cooling processes. However, when the four transformation temperatures of the samples are consolidated into the two graphs as shown in Figure 4, it can be observed that the  $M_f$  and  $A_s$  temperatures of the samples are very different from that of the NiTi ingot. Nonetheless, the  $M_s$  and  $A_r$  temperatures of the samples are similar to the  $M_s$  and  $A_r$  temperatures of the NiTi ingot and NiTi powder. This result would mean that there is a widening of the phase transformation temperature ranges from both martensite to austenite and from austenite back to martensite. For instance, the

ingot's microstructure starts to transform from austenite at 53 °C and finishes the transformation to martensite at 34 °C. As for the sample shown in Figure 3, its microstructure transforms from austenite at 49 °C and complete the transformation to martensite at 19 °C.

Another observation made is that the samples fabricated with a laser power of 50 W have more consistent transformation temperatures than the samples fabricated using 60 W. The reason for this phenomenon is not known yet and further study is required to understand the cause of this occurrence.

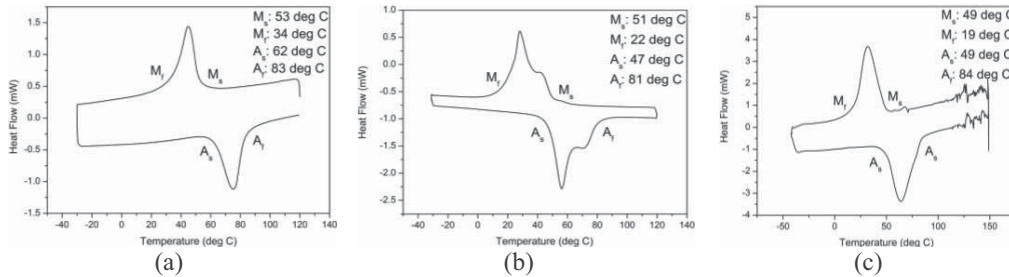


Figure 3. Transformation temperatures of (a) NiTi ingot, (b) NiTi powder and (c) 2D NiTi sample (laser power of 50 W, laser scanning speed of 3900 mm/s).

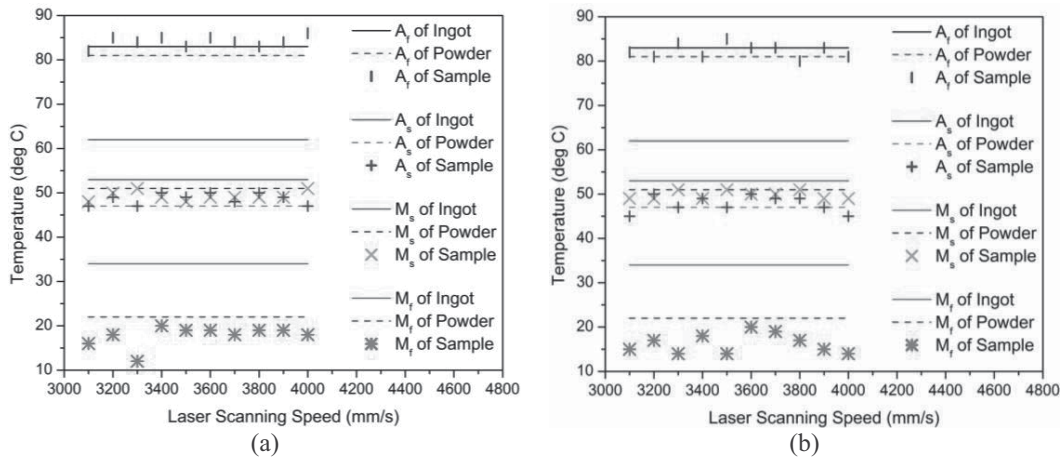


Figure 4. Comparison of the transformation temperatures of the NiTi ingot, NiTi powder, fabricated NiTi samples with (a) laser power 50 W and (b) laser power 60 W.

### CONCLUSION

In this paper, SLM was used to fabricate 2D NiTi samples from NiTi powder with laser power and laser scanning speed as the variable parameters. Density measurement was conducted on the samples and twenty of them with the highest bulk densities and relative densities and lowest closed porosities were chosen for the DSC testing. The results obtained from these tests are as follow:

1. The twenty samples with highest bulk and relative densities and lowest closed porosities displayed the presence of phase transformation during the heating and cooling processes.
2. Both the phase transformation temperature ranges from martensite to austenite and from austenite to martensite have widened after fabrication by SLM.
3. Samples that were fabricated with a laser power of 50 W exhibited more consistent transformation temperatures than the samples fabricated using 60 W.

## ACKNOWLEDGMENTS

The authors would like to express their gratitude to the funding provided by National Research Foundation, Singapore Centre for 3D Printing (SC3DP), School of Mechanical and Aerospace Engineering (MAE), Nanyang Technological University (NTU). The authors are also thankful for the support given by the MAE, NTU through a Tier 1 project, and by the Institute of Sports Research (ISR at NTU).

## REFERENCES

- Bormann, T., Schumacher, R., Muller, B., Mertmann, M., & Wild, M. d. (2012). Tailoring Selective Laser Melting process parameters for NiTi implants. *Journal of Materials Engineering and Performance*, 21.
- Chua, C. K., & Leong, K. F. (2014). *3D printing and additive manufacturing: Principles and applications* (A. Yun Ed. 4th ed.). Singapore: World Scientific Publishing Co. Pte. Ltd.
- Dadbakhsh, S., Speirs, M., Kruth, J.-P., Schrooten, J., Luyten, J., & Humbeeck, J. V. (2014). Effect of SLM parameters on transformation temperatures of shape memory nickel titanium parts. *Advanced Engineering Materials*, 16(9).
- Elahinia, M. H., Hashemi, M., Tabesh, M., & Bhaduri, S. B. (2012). Manufacturing and processing of NiTi implants: A review. *Progress in Materials Science*, 57, 911-946.
- Fremont, M., & Miyazaki, S. (1996). *Shape memory alloys*. New York: Springer-Verlag Wien GmbH.
- Frenzel, J., George, E. P., Dlouhy, A., Somsen, C., Wagner, M. F.-X., & Eggeler, G. (2010). Influence of Ni on martensitic phase transformations in NiTi shape memory alloys. *Acta Materialia*, 58, 3444-3458.
- I., S., I., Y., & I., S. (2012). Direct Selective Laser Melting of nitinol powder. *Physics Procedia*, 39, 447-454.
- K. Weinert, & Petzoldt, V. (2004). Machining of NiTi based shape memory alloys. *Materials Science and Engineering A*, 378, 180-184.
- Khoo, Z. X., Teoh, J. E. M., Liu, Y., Chua, C. K., Yang, S., An, J., . . . Yeong, W. Y. (2015). 3D printing of smart materials: A review on recent progresses in 4D printing. *Virtual and Physical Prototyping*, 10(3), 103-122.
- Meier, H., Haberland, C., & Frenzel, J. (2012). Structural and functional properties of NiTi shape memory alloys produced by Selective Laser Melting. *Innovative Developments in Virtual and Physical Prototyping*.
- Meier, H., Haberland, C., Frenzel, J., & Zarnetta, R. (2009). *Selective Laser Melting of NiTi shape memory components*. Paper presented at the Advanced Research in Virtual and Rapid Prototyping, Leiria, Portugal.
- Sanusi, K. O., Ayodele, O. L., & Khan, M. T. E. (2014). A concise review of the applications of NiTi shape-memory alloys in composite materials. *South African Journal of Science*, 110(7/8), 1-5.
- Sharma, N., Raj, T., & Jangra, K. K. (2015). Applications of nickel-titanium alloy. *Journal of Engineering and Technology*, 5(1), 1-7.
- Shishkovsky, I. V., Yadroitsev, I. A., & Smurov, I. Y. (2013). Manufacturing three-dimensional nickel titanium articles using layer-by-layer laser-melting technology. *Technical Physics Letters*, 39(12), 1081-1084.
- Zhang, B., Chen, J., & Coddet, C. (2013). Microstructure and transformation behavior of in-situ shape memory alloys by Selective Laser Melting Ti-Ni mixed powder. *Journal of Materials Science and Technology*, 29(9), 863-867.